

From Lattice QCD to Ultracold Atoms and Graphene: Accelerating the Monte Carlo approach to many-fermion physics

J. E. Drut¹ and T. A. Lähde²

¹Theoretical Division, Los Alamos National Laboratory,
Los Alamos, NM 87545, USA

²Helsinki Institute of Physics and Department of Applied Physics,
Aalto University, FI-00076 Aalto, Espoo, Finland

Email: jdrut@lanl.gov, talahde@gmail.com

Abstract. The lattice Monte Carlo study of quantum chromodynamics (lattice QCD) represents a tremendous investment in modern programming practices and efficient algorithms. We report on our efforts to adapt lattice QCD methods to other problems in many-fermion physics, in particular ultracold atoms at large scattering lengths and graphene.

1. Introduction

Many systems in condensed matter and low-energy nuclear physics are known to be well described by relatively simple Hamiltonians that often represent complicated, nonperturbative many-body dynamics. Examples include graphene (whose low-energy theory is closely related to strongly coupled quantum electrodynamics), high- T_c superconductors (described by the Hubbard model in two spatial dimensions), and ultracold atoms in the BCS-BEC crossover as well as dilute neutron matter (both captured by a nonrelativistic Hamiltonian with a zero-range interaction). While a qualitative understanding of such systems is often achievable with mean-field methods, a reliable *quantitative* description, aimed at predicting critical temperatures, couplings, and thermodynamic or transport properties, should preferentially resort to nonperturbative ab initio approaches such as quantum Monte Carlo (QMC), where the uncertainties are either systematic or statistical, yet fully controllable.

During the past three decades, the field of lattice QCD has witnessed a tremendous development toward algorithms where the scaling of the computation time with the size of the problem is considerably improved over older, more conventional algorithms. Our aim is to evidence the efficiency and utility of lattice QCD methods to practitioners in the condensed matter and ultracold atom communities, as well as to provide an overview of our recent results. In Sections 2 and 3, we discuss the application and performance of lattice QCD algorithms to ultracold Fermi gases and graphene, respectively. Section 4 provides a concluding summary of the physical results obtained so far.

2. From lattice QCD to ultracold Fermi gases

The starting point of studies of the equilibrium thermodynamics of classical or quantum systems is the grand canonical partition function \mathcal{Z} . In the case of spin-1/2 fermions with a local two-body interaction, we have

$$\mathcal{Z} \equiv \text{Tr} \exp[-\beta(\hat{H} - \mu\hat{N})] = \int \mathcal{D}\sigma (\det M[\sigma])^2 \exp(-S_g[\sigma]), \quad (1)$$

where $\hat{H} \equiv \hat{K} + \hat{V}$ is the Hamiltonian, \hat{K} the kinetic energy operator, \hat{V} the interaction operator,

and \hat{N} the particle number operator. This results from discretization of the imaginary-time dimension of extent τ into N_τ slices, followed by a Hubbard-Stratonovich (HS) transformation with auxiliary field $\sigma(\mathbf{x}, \tau)$ to represent the interaction. The fermion matrix M is given by

$$M \equiv \begin{pmatrix} \mathbb{1} & 0 & 0 & 0 & \dots & B_{N_\tau} \\ -B_1 & \mathbb{1} & 0 & 0 & \dots & 0 \\ 0 & -B_2 & \mathbb{1} & 0 & \dots & 0 \\ \vdots & \vdots & \vdots & \vdots & \vdots & \vdots \\ 0 & 0 & \dots & -B_{N_\tau-2} & \mathbb{1} & 0 \\ 0 & 0 & \dots & 0 & -B_{N_\tau-1} & \mathbb{1} \end{pmatrix}, \quad B_j \equiv \exp(-\tau K) \exp(-\tau V[\sigma_j]), \quad (2)$$

with $S_g[\sigma]$ a local action that depends on the original interaction as well as on the choice of HS transformation, as does the form of the auxiliary potential $V[\sigma]$. As our system is taken to be spin-symmetric, $M \equiv M_\uparrow = M_\downarrow$, and therefore the fermion sign problem is absent provided the interaction \hat{V} is attractive. The probability that defines the Markov chain in the configuration space of σ is then given by $P[\sigma] = (\det M[\sigma])^2 \exp(-S_g[\sigma]) \equiv \exp(-S_{\text{eff}}[\sigma])$, such that the problem of performing many-fermion QMC calculations is reduced to that of sampling the auxiliary field σ according to $P[\sigma]$ with efficient decorrelation.

A straightforward way of sampling is via the Metropolis accept/reject algorithm, with localized random updates of the field σ . This simple algorithm is referred to as determinantal Monte Carlo (DMC). Since random global changes have a negligible acceptance rate, DMC is not efficient at exploring the configuration space but does nevertheless possess a number of useful properties. For instance, DMC is very fast for small lattices of spatial extent between $N_x = 4$ and $N_x = 8$, as well as for low-dimensional problems. Also, since DMC allows for a two-valued discrete auxiliary field σ , disk and memory requirements are typically small as well.

A first step toward improved performance involves the hybrid Monte Carlo (HMC) algorithm. This combines the molecular dynamics (MD) evolution of σ in configuration space with a Metropolis accept/reject step. The MD Hamiltonian $\mathcal{H} = \pi^2/2 + S_{\text{eff}}[\sigma]$ defines equations of motion

$$\dot{\sigma} = \frac{\delta \mathcal{H}}{\delta \pi} = \pi, \quad \dot{\pi}_i = -\frac{\delta \mathcal{H}}{\delta \sigma_i} \equiv F_i[\sigma], \quad (3)$$

which should be integrated between regular updates of the random Gaussian momentum π using a reversible and area-preserving method. While we have introduced a new variable π , its path integral factors out from the original problem, such that it has no net effect on the probability density under study.

We refer to the approach where the fermion determinant enters the action S_{eff} directly as determinantal hybrid Monte Carlo (DHMC). This algorithm is efficient at intermediate lattice

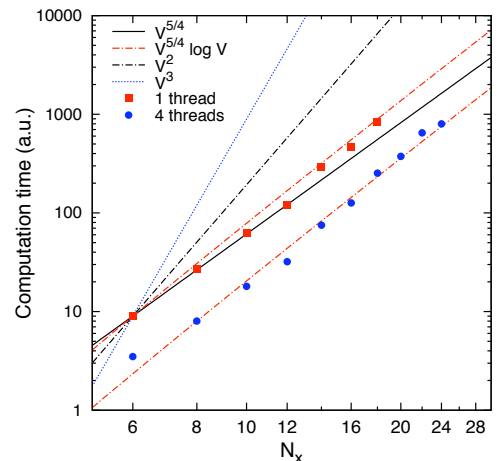


Figure 1: Timing of the ϕ -algorithm as applied to the unitary Fermi gas, in log-log scale, as a function of N_x at fixed N_τ . Red squares show results on a single CPU core, blue squares for 4 OpenMP threads.

volumes, in part because the calculation of $\det M = \det(\mathbb{1} + U)$, where $U \equiv \prod_{n=N_\tau}^1 B_n$, scales linearly with N_τ , and in part because the evaluation of $F_i[\sigma]$ involves the calculation of $(\mathbb{1} + U)^{-1}$, which is a dense matrix no larger than $N_x^3 \times N_x^3$. Because of the global MD updates, the scaling of DHMC is superior to DMC, although the prefactor in the scaling law is larger.

At sufficiently large N_x , scaling and memory limitations make the DHMC approach increasingly impractical, in which case “matrix-free” algorithms such as the “ ϕ -algorithm” variant of HMC may become better options. In the ϕ -algorithm, which is the main workhorse of modern Lattice QCD calculations, the fermion determinant and force $F[\sigma]$ are computed stochastically using the “pseudofermion” representation

$$(\det M[\sigma])^2 \propto \int \mathcal{D}\varphi^\dagger D\varphi \exp\left(-S_{\text{pf}}[\varphi^\dagger, \varphi, \sigma]\right), \quad S_{\text{pf}} = \int d^4x \varphi^\dagger (M[\sigma]^T M[\sigma])^{-1} \varphi, \quad (4)$$

for which the MD equations are obtained by substituting $S_{\text{eff}} \rightarrow S_g + S_{\text{pf}}$. Since the ϕ -algorithm allows for iterative conjugate gradient (CG) inversion involving the repeated application of $M[\sigma]$ to a given vector, the storage requirements are much reduced and the scaling properties further improved. However, since CG is sensitive to the condition number of $M^T M$, which is considerably more ill-conditioned than M , the prefactor of the scaling law can become prohibitively large at low temperatures (*i.e.* at large N_τ). Nevertheless, this approach is promising in conjunction with advanced preconditioning methods such as those based on Chebyshev polynomials.

In Fig. 1 we present the results of our first scaling tests. As our data indicates, preconditioned HMC scales approximately as $\sim V^{5/4}$ (the $\log V$ correction is due to the use of FFT when applying the matrix M). Other algorithms, such as DMC or diagrammatic Monte Carlo, scale approximately as $\sim V^3$ and $\sim V^2$, respectively. Figure 2 (left panel) shows our results on the first fully nonperturbative and ab initio calculation of Tan’s contact [9] as a function of temperature, obtained with the DHMC algorithm outlined above. In that work [10], we determined the Tan contact was from the large momentum tail of the momentum distribution, which we show in Fig. 2, multiplied by $3\pi^2(k/k_F)^4$.

3. Graphene and lattice Monte Carlo

At low energies, graphene is described by Dirac quasiparticles interacting via an instantaneous Coulomb interaction. The Euclidean action of this theory is $S_E = S_E^g + S_E^f$, where

$$S_E^g = \frac{1}{2g^2} \int d^3x dt (\partial_i A_0)^2 \quad (5)$$

is the gauge component. Here A_0 is a Coulomb field in $(3 + 1)$ dimensions, with $g^2 \equiv e^2/\epsilon_0$ for graphene in vacuum (suspended graphene). The fermion component is

$$S_E^f = \sum_{a=1}^{N_f} \int d^2x dt \bar{\psi}_a D[A_0] \psi_a, \quad D[A_0] = \gamma_0(\partial_0 + iA_0) + v\gamma_i\partial_i, \quad i = 1, 2, \quad (6)$$

with ψ_a a four-component Dirac field in $(2 + 1)$ dimensions. The spinor structure accounts for quasiparticle excitations on the two triangular sublattices, around the two inequivalent Dirac points. In graphene monolayers, $N_f = 2$ owing to electronic spin, while $N_f = 4$ is related to a graphene bilayer. The partition function of the low-energy theory of graphene is

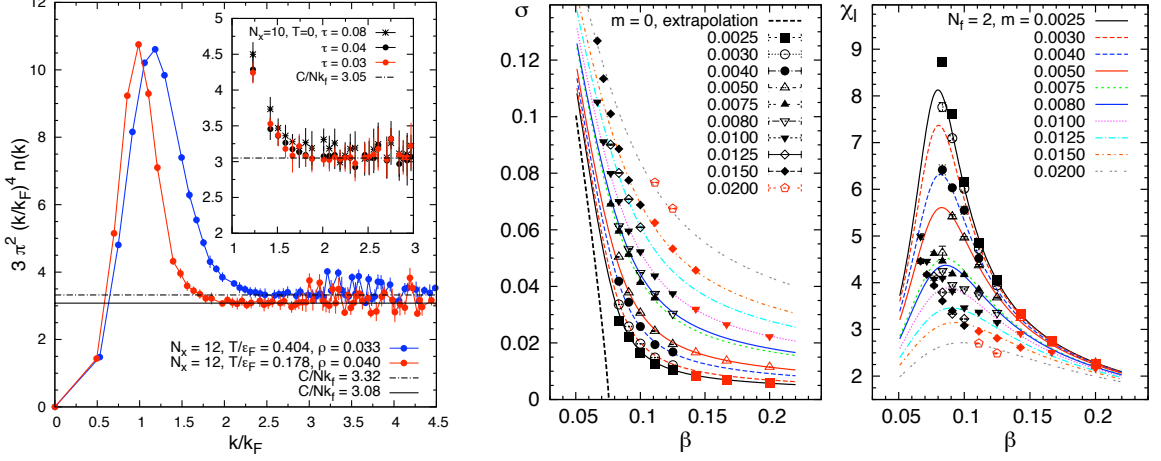


Figure 2: Physics highlights from our HMC calculations. Left: extraction of the Tan contact from the momentum distribution of a two-component Fermi gas [10]. Right: chiral condensate and susceptibility in the low-energy theory of graphene [8].

$$\mathcal{Z} = \int \mathcal{D}A_0 \mathcal{D}\psi \mathcal{D}\bar{\psi} \exp(-S_E[\bar{\psi}_a, \psi_a, A_0]), \quad (7)$$

where S_E is quadratic in the ψ_a . It is thus possible to integrate out the fermionic degrees of freedom, giving an “effective” gauge action

$$\mathcal{Z} = \int \mathcal{D}A_0 \exp(-S_{\text{eff}}[A_0]), \quad S_{\text{eff}}[A_0] = -N_f \ln \det(D[A_0]) + S_E^g[A_0], \quad (8)$$

where $P[A_0] \equiv \exp(-S_{\text{eff}}[A_0]) > 0$ defines a positive definite probability measure. However, the positivity of P breaks down in the presence of a chemical potential, as in lattice QCD. As in the ultracold atom problem of the previous section, we may implement choose to implement algorithms that involve the determinant directly or through a pseudofermion representation. The latter approach is known to be the most efficient for this class of problem.

As in lattice QCD, the inclusion of dynamical fermions in graphene is a notoriously difficult problem because of issues with chiral symmetry and fermion species doubling (for an overview, see citeRothe, Chapter 4). The “staggered” fermion representation [2] is well suited to the study of spontaneous chiral symmetry breaking, as it yields the correct number of degrees of freedom while also partially preserving chiral symmetry at finite lattice spacing. The action of a single staggered flavor is

$$S_E^f[\bar{\chi}, \chi, \theta] = \sum_{\mathbf{n}, \mathbf{m}} \bar{\chi}_{\mathbf{n}} D_{\mathbf{n}, \mathbf{m}}[\theta] \chi_{\mathbf{m}}, \quad (9)$$

where the staggered Dirac operator [8] is given by

$$D_{\mathbf{n}, \mathbf{m}}[\theta] = \frac{1}{2}(\delta_{\mathbf{n}+\mathbf{e}_0, \mathbf{m}} U_{\mathbf{n}} - \delta_{\mathbf{n}-\mathbf{e}_0, \mathbf{m}} U_{\mathbf{m}}^\dagger) + \frac{v}{2} \sum_i \eta_{\mathbf{n}}^i (\delta_{\mathbf{n}+\mathbf{e}_i, \mathbf{m}} - \delta_{\mathbf{n}-\mathbf{e}_i, \mathbf{m}}) + m_0 \delta_{\mathbf{n}, \mathbf{m}}. \quad (10)$$

We have determined the critical Coulomb coupling for spontaneous chiral symmetry breaking (i.e., gap formation) by evaluating the condensate $\langle \bar{\psi}\psi \rangle$ as a function of $\beta \equiv v/g^2$. The

staggered lattice action does not retain the full $U(4)$ chiral symmetry of the original graphene action at finite lattice spacing. As shown in [4], only a subgroup $U(1)\times U(1)$ remains upon discretization. Spontaneous condensation of $\bar{\chi}\chi$, or equivalently the introduction of a parity invariant mass term, reduces this symmetry to $U(1)$. In the staggered fermion formulation, the transition to a gapped phase is associated with this chiral symmetry-breaking pattern.

4. Summary

Recent developments in the field of lattice QCD have produced a variety of efficient algorithms and numerical methods to tackle large-scale many-fermion problems. While these methods have proven their worth in that field, until recently their applicability to problems in other areas, such as condensed matter and atomic physics, or even to other problems within nuclear physics, remained poorly understood.

Our work shows that it is possible and beneficial to apply algorithms involving HMC updates to current and relevant problems in ultracold atoms and graphene, since the improved scaling properties allow for the efficient study of large systems. Simultaneously, we have shown that gaining access to larger system sizes provides new and valuable physical insight. Further developments we are currently exploring include preconditioning strategies tailored to nonrelativistic Hamiltonians, as well as GPU implementations of HMC.

Acknowledgments

We thank A. Bulgac, J. A. Carlson, and R. J. Furnstahl for encouragement during the early stages of these investigations. Our work was partially supported by U.S. DOE Grants No. DE-FG02-00ER41132 and DE-AC02-05CH11231, UNEDF SciDAC Collaboration Grant No. DE-FC02-09ER41586 and NSF Grant No. PHY-0653312. This study was also supported in part by the Academy of Finland through its Centers of Excellence Program (2006 - 2011), the Vilho, Yrjö, and Kalle Väisälä Foundation of the Finnish Academy of Science and Letters, and the Waldemar von Frenckell and Magnus Ehrnrooth Foundations of the Finnish Society of Sciences and Letters.

References

- [1] N. Metropolis et al., *J. Chem. Phys.* **21**, 1087 (1953).
- [2] J. Kogut, L. Susskind, *Phys. Rev. D* **11**, 395 (1975); L. Susskind, *Ibid.* **16**, 3031 (1977); H. Kluberg-Stern, *Nucl. Phys. B* **220**, 447 (1983).
- [3] H. J. Rothe, *Lattice Gauge Theories - An Introduction*, 3rd ed., World Scientific (2005).
- [4] C. Burden, A. N. Burkitt, *Eur. Phys. Lett.* **3**, 545 (1987).
- [5] S. Duane *et al.*, *Phys. Lett. B* **195**, 216 (1987); S. Gottlieb *et al.*, *Phys. Rev. D* **35**, 2531 (1987).
- [6] K. Wendt, J. E. Drut, T. A. Lähde, *Comput. Phys. Commun.* (in press) [arXiv:1007.3432].
- [7] T. Ten, J. E. Drut, T. A. Lähde, [arXiv:1008.3647].
- [8] J. E. Drut, T. A. Lähde, *Phys. Rev. Lett.* **102**, 026802 (2009); *Phys. Rev. B* **79**, 165425 (2009); *Ibid.* **79**, 241405(R) (2009).
- [9] S. Tan, *Ann. Phys.* **323**, 2952 (2008); *Ibid.* **323**, 2971 (2008); *Ibid.* **323**, 2987 (2008).
- [10] J. E. Drut, T. A. Lähde, T. Ten, *Phys. Rev. Lett.* **106**, 205302 (2011).